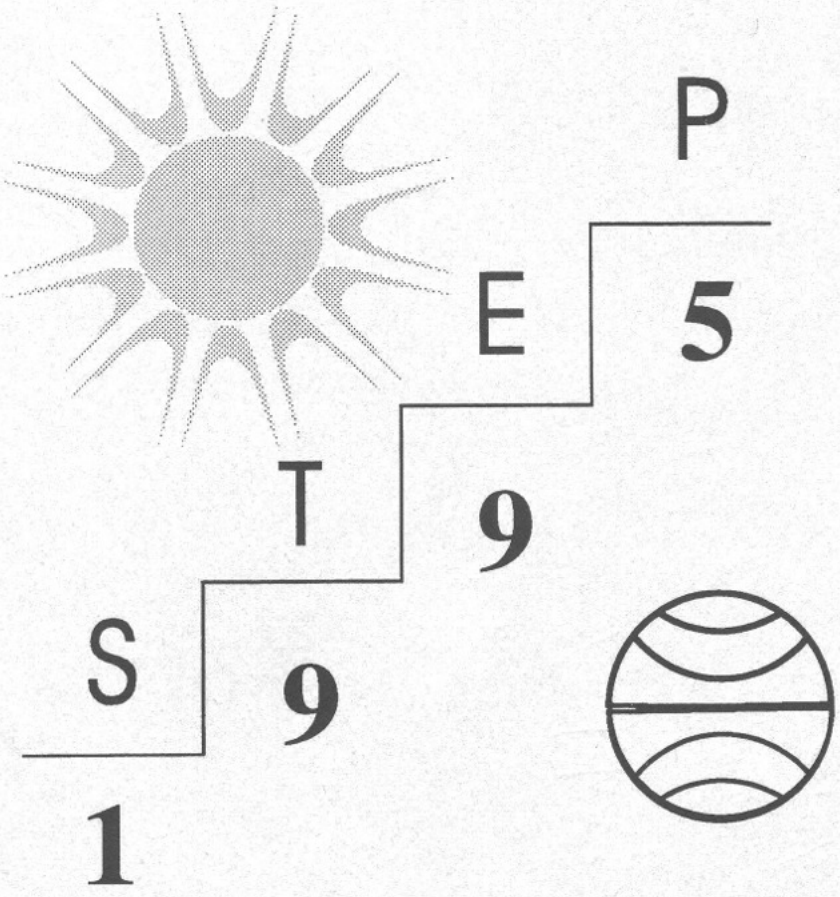

Conference on Solar and Terrestial Physics

Jointly Organised by the Department of Physics
and Mathematical Physics of
The University of Adelaide
and
The High Frequency Radar Division
of the DSTO Salisbury

25 - 29 September 1995

UNIVERSITY OF ADELAIDE
Adelaide, South Australia

STEP 1995 PROGRAM

SEPTEMBER 25 (MONDAY)

9:00	Registration and Poster Setup	
10:00	Welcome R A Vincent	
10:15	Morning Tea	
Session 1	**CHAIR M Golley**	
10:45	**Reid I M** (Tutorial) Radar Measurements of the Atmosphere (0-100km)	1
11:30	**Klekociuk A R, Innis J, Morris R J, Vincent R A, Reid I M** Doppler Performance of the Lidar for Davis, Antarctica	5
11:45	**Valentic T A, Avery J P, Avery S K, Cevera M A, Vincent R A, Reid I M, Elford W G** A Comparison of Meteor Radar Systems at Buckland Park	7
12:00	LUNCH	
Session 2	**CHAIR I M Reid**	
13:00	**Downey A, Fraser P, Atkinson R, Lehmann P** (Tutorial) The Antarctic Ozone Hole (a brief discussion and a look at the 1994 event)	11
13:45	**Innis J L, Greet P A, Dyson P L** Vertical motions in the thermosphere near the Auroral Oval/Polar Cap boundary above Mawson, Antarctica	14
14:00	**Murphy D J** Momentum Fluxes over Adelaide during the Two-Day wave, 1987	17
14:15	**Vandepeer B G W, Reid I M** Observations with the modified Bribie Island MF radar	21
14:30	Afternoon Tea	
15:00	**Russell C J, Dyson P L, Bennett J A** Numerical Ray Tracing Studies of Ionospheric Propagation	23
15:15	**Elford W G, Taylor A D** Measurement of electron densities in the lower ionosphere from Faraday rotation of radar meteor echoes	27
15:30	**Hibberd F H** Annual and Semi-annual Variations in Sq and Thermospheric Temperature.	30

15:45 **Parkinson M L, Smith P R, Dyson P L, Scali J L, Bullet T** 34
Analysis of angle-of-arrival ambiguities for HF spaced-antenna drift measurements

16:00 **Baker P W** 38
Low Latitude Low-VHF Skywave Propagation

16:15 **Short Break**

16:30 **Breed A M, Vandenberg A-M, Goodwin G L, Silby J H, Lynn K J W, Essex E A** 39
Australian Ionospheric Slab Thickness Determined from GPS Satellite Observations.

16:45 **Dubovinsky M, Monselesan D P, Wilkinson P, Dyson P L, Smith P R, Schneider D, Morris R J** 43
Comparison of Empirical Model Predictions with Automatically and Manually Scaled Ionospheric Parameters for the Polar Cap Station of Casey

17:00 **Stankov S M** 47
On Modelling the Light-Ion Densities in the Ionosphere

17:15 **Meehan D** 51
Diurnal and Seasonal Variation of Backscattered Returns as Seen with A High Frequency Radar

SEPTEMBER 26 (TUESDAY)

Session 3 **CHAIR B J Fraser**

9:00 **Tsuda T (Invited)** 55
Observations of Middle Atmosphere Dynamics in Equatorial Indonesia with Radars and Radiosondes

9:30 **Cervera M A, Elford W G, Steel D I** 59
A novel radar technique for the determination of meteor speeds and its significance in the interpretation of HF/ VHF meteor backscatter

9:45 **Holdsworth D A, Reid I M, Briggs B H, Vincent R A** 63
Intercomparisons of various spaced antenna analysis techniques

10:00 **Percival D J** 67
Short-term Forecasting of HF Propagation Conditions using Time Series Analysis

10:15 **Morning Tea**

10:45 **Vincent R A, Morris R J, Murphy D J** 71
MF Radar Studies of the Antarctic Mesosphere at Davis: First Results

11:00 **Watkins B J** 75
Incoherent-scatter radar observations of metallic ion layers

11:15 **Dyson P L (Tutorial)** 76
The Tasman International Geospace Environment Radar (TIGER)

12:00 **TIGER Meeting**

12:45 **LUNCH**

Session 4 **CHAIR P L Dyson**

13:30 **Clarke R H, Lynn K J W, Kettler D** 80
An Update on DSTO's Low Latitude Ionospheric Sounding Program (LLISP)

13:45 **Caruana J** 81
Availability Computations using ASAPS

14:00 **Lingard D M** 85
Transformation of Beam Steering Data to Allow Measurement of D-region Winds using the Spaced Antenna Technique

14:15 **Du J H, Stening R J** 89
Characteristics of Ionospheric Flux Tube Integrated Conductivity

14:30 **Afternoon Tea**

15:00 **Hecht J H (invited)** 93
Measuring the Nightglow: One Persons Noise is Another Persons Signal

15:30 **Whitehead J D** 94
Modeling of Instabilities in Mid-Latitude Sporadic-E

15:45 **Greet P A, Dyson P L, Morris R J** 95
Mawson Fabry-Perot Spectrometer Data Archive

16:00 **Ables S T, Fraser B J, Olson J V, Hansen H J** 99
Phase Analysis for Conjugate ULF Pulsations in the 1-10 mHz Range at Cusp Latitudes

16:15 **Dowdell G G, Hu Y D, Fraser B J** 100
A Ray Tracing Study of Electromagnetic Ion Cyclotron Waves in the Middle Magnetosphere

16:30 **Eckermann S D, Marks C J** 101
Ray Model of Gravity Wave-Tidal Interactions in the Mesosphere and Lower Thermosphere

16:45 **Wilson M J** 105
Northern Auroral Observations using a Southern Hemisphere Mid-Latitude Backscatter Sounder

17:00 **Harris T J, Wilson M J** 109
Variability of Auroral Backscatter Observed by OTHR

17:15 **Essex E A** 113
Ionospheric Storms and the Plasmasphere

SEPTEMBER 27 (WEDNESDAY)

Session 5 **CHAIR R J Morris**

9:00 **Fraser B J (Tutorial)** 117
ULF Waves in the Earth's Magnetosphere

9:45 **Marshall R** 118
Real-Time Applications of Geomagnetic Pulsation data

10:00 **McCreadie H, Butcher E C** 122
Night-Time Annual Variations of the Geomagnetic Field

10:15 **Morning Tea**

10:45 **Hu Y D, Fraser B J** 126
Nonlinear Modulation of Electromagnetic Ion Cyclotron Waves

11:00 **Phanivong B, Dyson P L, Bennett J A, Finn A** 127
Electron Density Profiles and Propagation Characteristics Determined by Inversion of Oblique and Vertical Incidence Ionograms

11:15 **Bennett J A, Nguyen X L, Dyson P L** 131
Interpolation of Oblique Ionograms for Co-ordinate Registration

11:30 **Barnes R** 135
Calculation of the Faraday Rotation in the Ionosphere

11:45 **Thomas R M, Harris T J, Whitington M J, Blesing R G** 139
The Jindalee Synoptic Spread Clutter Database

12:00 **LUNCH**

12:30 Bus leaves for Winery Tour

19:00 Conferece Dinner

SEPTEMBER 28 (THURSDAY)

Session 6 — **CHAIR R A Vincent**

9:00 **Tsunoda R (Invited)** 143

9:30 **Hansen H J, Fraser B J, Menk F W, Morris R J** 144
The Propagation of Pc3 Wave Energy Through The Dayside Magnetopause

9:45 **Fraser B J, Lee S H, Waters C L, Samson J C** 145
Field Line Resonance in the Magnetosphere: Integration of Ground and Satellite Observations

10:00 **Neudegg D A, Fraser B J, Menk F W, Hansen H J, Burns G B, Morris R J, Underwood M J** 146
Observations of Geospace coupling near the Austral Cusp/Cleft region

10:15 **Morning Tea**

10:45 **Chaston C C, Hu Y D, Fraser B J** 147
The Quasi-linear Evolution of Particle Distributions and Ion Cyclotron Waves in the Near Earth Plasma Sheet Boundary layer

11:00 **May P T, Rajopadhyaya D K** 148
Wind Profiler Observations of Vertical Motion and Precipitation Microphysics of a Tropical Squall Line

11:15 **Abramovich Yu I, Anderson S J, Frazer G J, Solomon I S D** 152
Measurement and Interpretation of Phase Fluctuations in HF Radar Echoes Propagated via Sporadic E Layers

11:30 **Coleman C J** 156
Backscatter Ionogram Simulation

11:45 **Menk F W** 160
Response of the Low Latitude ULF Spectrum to Solar Wind Input

12:00 **STEP AGM**

12:45 **LUNCH**

Session 7 — **CHAIR P Wilkinson**

13:30 **Kennewell J A (Tutorial)** 161
Background to Space Weather - A Tutorial

14:15 **Igarashi K** 165
A New Ionospheric Observation Data Network and MF Radar Chain in Japan

14:30 **Li Y** 169
Forecasting the features of sunspot cycle 23

14:45 **Gizon L** 173
Can we see the back of the Sun?

Session 8 **CHAIR P A Greet**

15:00 Poster Preview (1 minute Talk)

15:45 Poster Session

SEPTEMBER 29 (FRIDAY)

Session 9 **CHAIR J Whitehead**

9:00 **Stening R J (Invited)** 177
The Ionospheric Dynamo and the Sq Current System

9:30 **Mudge L** 181
Optimum configurations of HFDF single station location networks

9:45 **Waters C L** 182
Ground based diagnostic of Plasmatrough plasma density

10:00 **Dunlop I S, Menk F W, Marshall R A, Waters C L** 183
Spatial Characteristics of ULF Geomagnetic Pulsations Observed in the Low Latitude Ionosphere

10:15 Morning Tea

10:45 **Breed A M, Vandenberg A-M, Goodwin G L, Silby J H, Essex E A** 184
Protonospheric Effects on GPS Position Determination

11:00 **Lynn K J W, Clarke R H, Finn R A** 188
Ionospheric Variability at Low Latitudes

11:15 **Smith P R, Monselesan D P, Dubovinsky M, Dyson P L, Morris R J** 189
Seasonal Changes in the Ionospheric Convection Pattern Observed at Casey, Antarctica

11:30 **Nelson G R** 193
An edge detector and its applications to the study of variability in backscatter Ionogram leading edges

11:45 **Tyler M A, Wilson M J** 197
HF Observations of Antipodean Backscatter Clutter

12:00 Close

12:30 Bus leaves for Buckland Park

On Modelling the Light-Ion Densities in the Ionosphere

S. M. Stankov *

School of Physics
The University of New South Wales
Sydney , NSW 2052 , Australia

Abstract

A steady-state theoretical model is used to obtain variations of the H^+/O^+ and He^+/O^+ density ratios in the upper ionosphere at middle latitudes. The model results are compared with the existing data from satellite measurements. Analytical formulae are constructed approximating the latitude and altitude variations of these ratios for direct use in the International Reference Ionosphere (IRI) model.

1. Introduction

Modelling the densities of the light ions, H^+ and He^+, for different geographic locations and various ionospheric conditions is a problem with two main aspects of difficulty. *First*, the experimental data (satellite, rocket, or ground-based) are too few to embrace the altitude variations of the light-ion densities with respect to local time, solar and geomagnetic activity, season, and latitude. This shortage restrains the validity of some empirical models to narrow ranges of the mentioned parameters. Moreover, the use of mass-spectrometer measurements generates the problem of calibration that impedes the use of data from different satellites. *Second*, the purely theoretical approach is not very helpful. The problems with the existing theoretical models for $n(H^+)$ and $n(He^+)$ are in the precise setting of boundary values and in the choice of an adequate neutral atmosphere model.

Here, a different approach to the modelling of the light-ion densities is proposed, combining the advantages of empirical and theoretical modelling. On both sides of the O^+-H^+ and O^+-He^+ transition heights the ratios $n(H^+)/n(O^+)$ and $n(He^+)/n(O^+)$ are calculated by using a steady-state mathematical model and the solutions are compared with satellite measurement data. Analytical formulae are constructed giving the altitude variations of the density ratios depending on dipole latitude. The theoretical model might then use an empirical model of transition levels to obtain the variations of the above density ratios due to local time, longitude, season, etc. A possible implementation of the constructed formulae in existing empirical models is discussed, e.g. for improving the IRI ion composition model.

---

* On leave from the Geophysical Institute, Bulgarian Academy of Sciences

2. Mathematical model

A steady-state mathematical model is used to calculate the density profiles of the O^+, H^+, and He^+ ions. In the model the equations of continuity, momentum, and energy balance are solved numerically along a given centred-dipole magnetic field line from a start altitude (~ 200 km) to an arbitrary upper altitude. The model is not self consistent and uses a number of quantities as input parameters - the neutral atmosphere, solar EUV flux, meridional component of the neutral wind, etc. As an extension of the steady-state model, an original numerical procedure is developed for determination of the boundary values in a self-consistent manner.

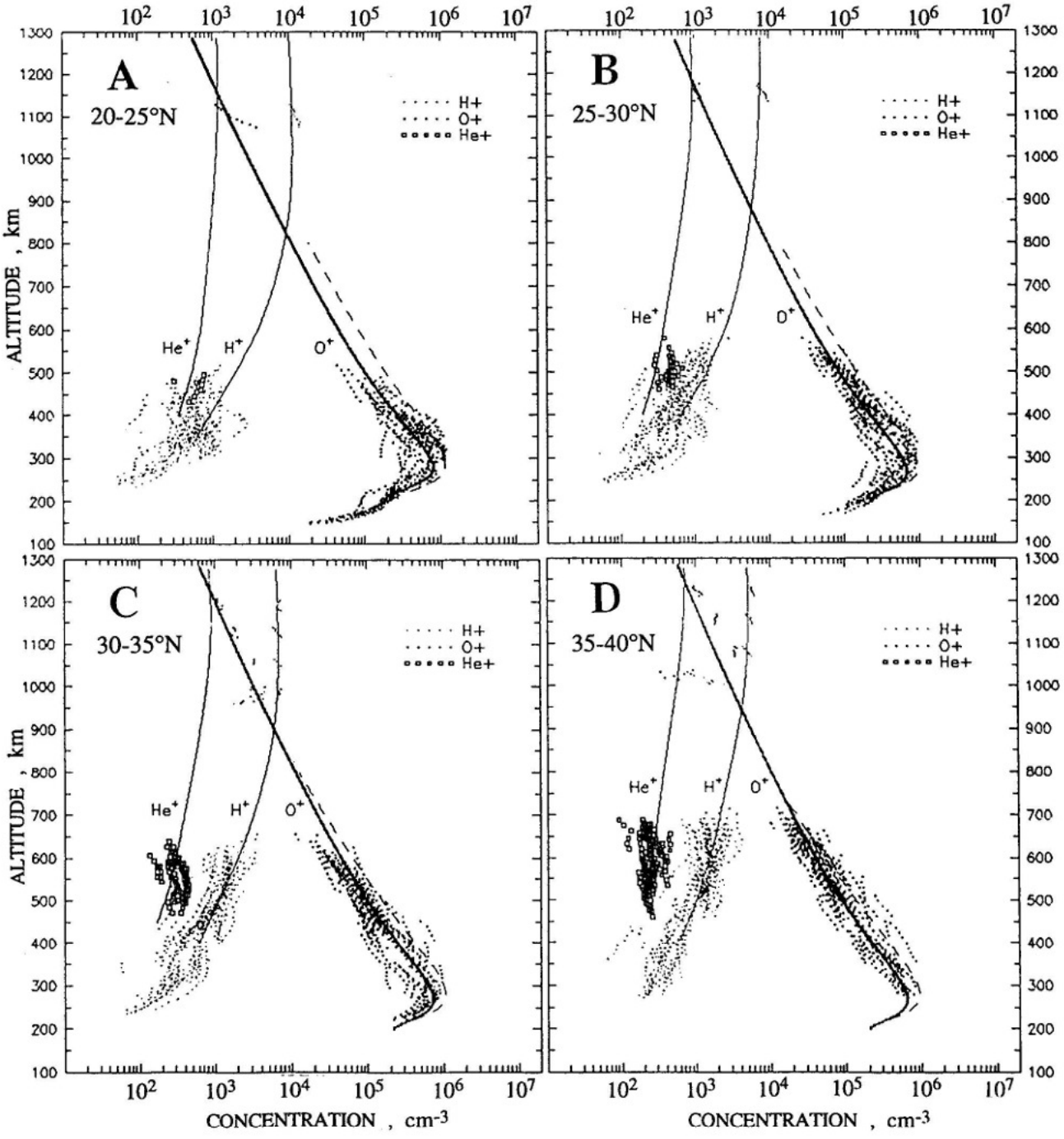

Fig.1 *Comparison between theoretical and measured densities*

3. Data base

Satellite data (O^+, H^+, He^+ ion concentration) from Atmosphere Explorer (AE-C) are used for comparison with the model's results. These data represent the equinox period, 1/09/1974-31/10/1974, daytime conditions (10.00-14.00 LT), low solar activity ($F_{10.7}$ = 90), and moderate geomagnetic activity (A_P=20). The data from all the longitudes and within the invariant latitude range 20-40°N are sorted into four groups (**Fig.1**) according to latitude: 20-25°, 25-30°, 30-35°, and 35-40°N. The O^+ densities cover the altitude range 150-700 km describing pretty well the noon O^+ profile in the F-region. Due to satellite evolution, the data from higher latitudes cover higher altitudes. There are just a few data between 900 and 1300 km height, but they are very important for comparing the theoretical profiles with the measurements at and above the transition levels. The H^+ and He^+ data are much more scattered than the O^+ data.

4. Comparison between model results and measurement data

Adopting the neutral atmosphere from MSIS-90, [3] , the O^+, H^+, He^+ density profiles are calculated for the same conditions as for the satellite measurements described above. The results are given on **Fig.1**. The dashed lines represent the O^+ profiles as calculated by using the initial value searching method and obviously exceed the measurements. New profiles are obtained (solid line) by a 5-10% decrease in the initial value of the electron temperature, T_e . The theoretical H^+ and He^+ profiles are corrected significantly by reducing the H and He neutral densities; this reduction is different for each of the four cases and generally varies between 2 and 5 times. The latter means that in MSIS those concentrations are higher but a correct estimation could be obtained if the exact production and loss rates were known.

5. Results: analytical formulae for H^+/O^+ and He^+/O^+ density ratios

Here only the method for obtaining the analytical formulae for the light-ion density ratios will be demonstrated by using the corrected result given above. First, the altitude variations of $n(H^+)/n(O^+)$ and $n(He^+)/n(O^+)$ are calculated for each of the latitude ranges. Thus, four altitude profiles of $n(H^+)/n(O^+)$ and four profiles of the $n(He^+)/n(O^+)$ ratio are obtained. After that, the four ratio profiles are used to derive a latitude dependence. Finally, the altitude and latitude ratio variations are approximated by the two-variable function

$$f_i(x, y) = a_i \, \boldsymbol{exp}\,(b_i y)\, x^{(c_i y + d_i)} \quad , \quad i=1,2$$

where x is the altitude, y is the dipole latitude, i=1 stands for $n(H^+)/n(O^+)$ and i=2 stands for $n(He^+)/n(O^+)$. The coefficients are

a_1=2.05149×10^{-19}	b_1=-0.184102	c_1=0.018306	d_1=6.59654
a_2=4.78135×10^{-16}	b_2=-0.455081	c_2=0.059176	d_2=5.11627

which are valid for the conditions stipulated above, i.e. equinox, noon, low solar activity, 20-40°N dipole latitude. Additional satellite data are needed to obtain coefficients for other conditions.

6. Discussion

The constructed analytical formulae are very useful for calculating H^+ and He^+ densities when the O^+ density is available. Thus, it might be used with existing empirical models to improve their ion composition part. For example, the most adequate ionospheric model to date, the IRI , shows the $n(H^+)/n(He^+)$ ratio to be almost constant with varying altitude, which in most of the cases is not valid. Generally, the IRI ion composition is not reliable. There are at least two reasons: *first*, the great variability of the light ion densities; and *second*, the limited data base (for example, no data from AE-C, AE-E, DE-2 satellites are considered, [1,2]). Thus, the use of results from a theoretical model based on satellite data is appropriate.

To extend the formulae to other conditions, additional data are needed. Also, a very helpful tool is the constructed empirical model of O^+-H^+ transition level, described in [4]. The global O^+-H^+ transition surface is based on OGO-6, Bulgaria-1300, Alouette-1, ISS-b, and other satellite measurement data. The transition-level variations are approximated by a fitting generalized polynomial which depends on the 5 parameters used in IRI, i.e. sunspot number, month, local time, dipole latitude, and longitude. The use of this empirical model is important for two main reasons. *First*, the O^+-H^+ transition level will serve as an anchor point, when theoretically calculating the density profile. Thus, the uncertainty in the adopted neutral atmosphere model will be overcome. The influence of the adopted atmosphere on the model results (especially during daytime) has been already analysed in [5] and a high sensitivity demonstrated. *Second*, the transition level model provides the important diurnal and longitudinal variations.

Acknowledgements

I am thankful to Prof. I. Kutiev for the useful discussions and Prof. R. J. Stening for carefully reading the manuscript.

References

[1] **D. Bilitza, K. Rawer, L. Bossy, T. Gulyaeva** (1993)
International Reference Ionosphere - Past, Present, and Future:
I. Electron Density
Adv. Space Res., vol.13, No.3, pp.(3)3-(3)13

[2] **D. Bilitza, K. Rawer, L. Bossy, T. Gulyaeva** (1993)
International Reference Ionosphere - Past, Present, and Future:
II. Plasma Temperatures, Ion Composition and Ion Drift
Adv. Space Res., vol.13, No.3, pp.(3)15-(3)23

[3] **A. E. Hedin** (1991)
Extension of the MSIS Thermospheric Model into the Middle and Lower Atmosphere
J. Geophys. Res., vol.96, No.A2, pp.1159-1172

[4] **I. Kutiev, S. M. Stankov, P. Marinov** (1994)
Analytical Expression of O^+-H^+ Transition Surface for Use in IRI
Adv. Space Res., vol.14, No.12, pp.(12)135-(12)138

[5] **I. Kutiev, S. M. Stankov** (1994)
Relative Abundance of H^+ and He^+ in the Outer Ionosphere
Adv. Space Res., vol.14, No.12, pp.(12)139-(12)141